CORROSION IN ACID GAS INJECTION SYSTEMS - PROJECT 101

Kevin S. Fisher, P.E. and Kenneth E. McIntush, P.E.
Trimeric Corporation
Buda, Texas, U.S.A.

Peter F. Ellis
Honeywell Corrosion Solutions
Houston, Texas, U.S.A.

ABSTRACT

Natural gas producers have needed to remove undesirable acid gas impurities such as hydrogen sulfide and carbon dioxide for many years. The separation of these acid gases from the natural gas ultimately produces a concentrated stream of acid gas which requires disposal. In recent decades, it has become more common to compress this gas to very high pressures and inject the stream into a suitable underground reservoir for disposal. More recently, carbon capture and sequestration (CCS) has become a potential means of reducing the release of greenhouse gases to the atmosphere. It, too, involves the compression, transportation and injection of high-pressure CO_2 fluids.

Due to the corrosive and toxic properties of these acid gases, and the need to contain and process them safely in high pressure systems, there is a need to understand how the corrosivity of these gases toward commonly used alloys of steel varies with the process conditions and the concentrations of potential impurities that may be present in the acid gas stream. The goal of this research project was to measure the corrosivity of various acid gas mixtures under conditions that are typical of commercial acid gas injection systems using laboratory autoclaves and test specimens. Of particular interest in this program was the effect of varying the temperature, relative water saturation, and concentration of hydrogen sulfide, oxygen, and methanol.

1.0 INTRODUCTION

Natural gas often contains impurities like H_2S and CO_2. To meet pipeline specifications, these impurities must be removed to acceptable levels. As a result, concentrated mixtures of H_2S and CO_2 (i.e., "acid gases") are generated. Often, acid gas is processed to convert the toxic H_2S to benign elemental sulfur, while the CO_2 is vented. However, increased "involuntary" production of elemental sulfur has resulted from the development of increasingly sour (i.e., containing more H_2S) oil and gas reservoirs. Also, there is greater sensitivity to venting CO_2 to the atmosphere. Thus, acid gas injection (AGI) is becoming a popular alternative to sulfur recovery for waste gases containing H_2S and CO_2, as sulfur production is avoided and CO_2 is not vented. Carbon capture and sequestration (CCS), involving the capture of CO_2 from flue gas, also reduces the release of CO_2 to the atmosphere.

When aqueous solvents are used to treat sour natural gas or flue gas, the raw acid gas is saturated with water. It is well known that both CO_2 and H_2S are corrosive to carbon steel when liquid water is present. The risk posed by corrosion is even greater when AGI is the disposal method, owing to the high pressures (several hundred to 2000+ psi) and high H_2S concentrations (~5+ mol%) involved. Consequently, it is of interest to understand the range of conditions under which pressurized acid gas may be corrosive.

Even a small leak of high-pressure, high-H_2S gas can have a significant impact, making it important to understand potential conditions under which the acid gas may be corrosive. Free water in acid gas injection systems is a significant potential safety issue, as wet acid gas is generally corrosive to carbon steel piping and injection tubulars.

The objective of this project was to collect corrosion data to better define safe operating envelopes and materials for AGI and CCS. In particular, the impact of temperature, water saturation and common impurities in the gas, including oxygen and methanol, was investigated.

Following an initial literature review of publically available data, a series of batch autoclave tests were performed which resulted in corrosion rate data for several commonly used types of steel, over a range of temperatures and compositions. This paper presents an overview of the research effort and results for this study. Details of the literature review, experimental procedures, and other specific test results can be found in the research report[1] published for this work.

2.0 TEST CONDITIONS

Table 1 shows the test conditions for the corrosion experiments in this study. Corrosion rates were measured using 30-day batch autoclave tests equipped with corrosion test specimens made of X65 carbon steel and Type 410 and 316L stainless steel alloys. Seventeen test runs were conducted at 1275 psig and either 75ºF (dense-phase CO_2) or 125ºF (supercritical CO_2). The relative water saturation of the gas was controlled at either 75% or 100%, and the composition of the gas varied to include levels of H_2S up to 5 mol% percent and oxygen up to 1 mol%, with the balance CO_2.

In all cases, the test specimens were located in the headspace of the autoclave with a small reservoir of humidifying liquid on the bottom of the autoclave. The humidifying liquid in five of the tests was distilled water, resulting in 100% relative saturation (RS) in the headspace. The RS is the actual vapor-phase moisture content divided by the saturation moisture concentration expressed as

a percent. Eight tests were performed in which the humidifying liquid was an NaCl/water slurry, resulting in an RS of 75 ± 3%. Four tests were conducted in the presence of a 20 wt% methanol solution. Unlike the preceding tests, the specimens in the methanol/water tests were intentionally splashed with the humidifying liquid.

Table 1. Summary of Test Conditions

Test #	Temp (F)	Solution	Relative Saturation (%)	Coupons splashed with solution	H_2S (mole %)	O_2 (mole %)
1	125	distilled water	100	Yes	0	0
2	125	distilled water	100	Yes	3.9	0
3	75	distilled water	100	Yes	0	0
4	75	distilled water	100	Yes	1.55	0
5	125	25% NaCl	75	Yes	5	0
6	75	25% NaCl	75	Yes	5	0
7	125	25% NaCl	75	No	5	0
8	125	distilled water	100	No	5	0
9	125	25% NaCl	75	No	0	0
10	75	25% NaCl	75	No	0	0
11	125	25% NaCl	75	No	0	1
12	75	25% NaCl	75	No	0	0
13	125	25% NaCl	75	No	0	1
14	75	20% MeOH	100	Yes	0	0
15	75	20% MeOH	100	Yes	5	0
16	75	20% MeOH	100	Yes	0	1
17	75	20% MeOH	100	Yes	5	1

3.0 EXPERIMENTAL METHODS

This section presents a summary of the experimental apparatus, corrosion specimens, and test procedures and methods for evaluating corrosion rates.

3.1 Autoclave Laboratory Apparatus

All of the testing for this program was performed using Honeywell's 5-L autoclaves rated for pressures up to 5000 psig at 550°F. The Alloy C-276 clad chambers of these autoclaves are 5 inches in diameter by 17 inches deep. Each autoclave is equipped with a gas inlet tube (dip tube) that extends to the bottom of the autoclave, a gas outlet tube, and an internal thermowell with thermocouple to control the temperature of the autoclave to within ± 5°F with external heater bands. Temperature and pressure were continuously monitored during the tests. Figure 1 shows one of these autoclaves.

The autoclaves were mechanically scrubbed with laboratory detergent prior to each test with H_2S. For tests without H_2S, the autoclaves were further decontaminated using a powerful oxidizing acid to remove any possible sulfides.

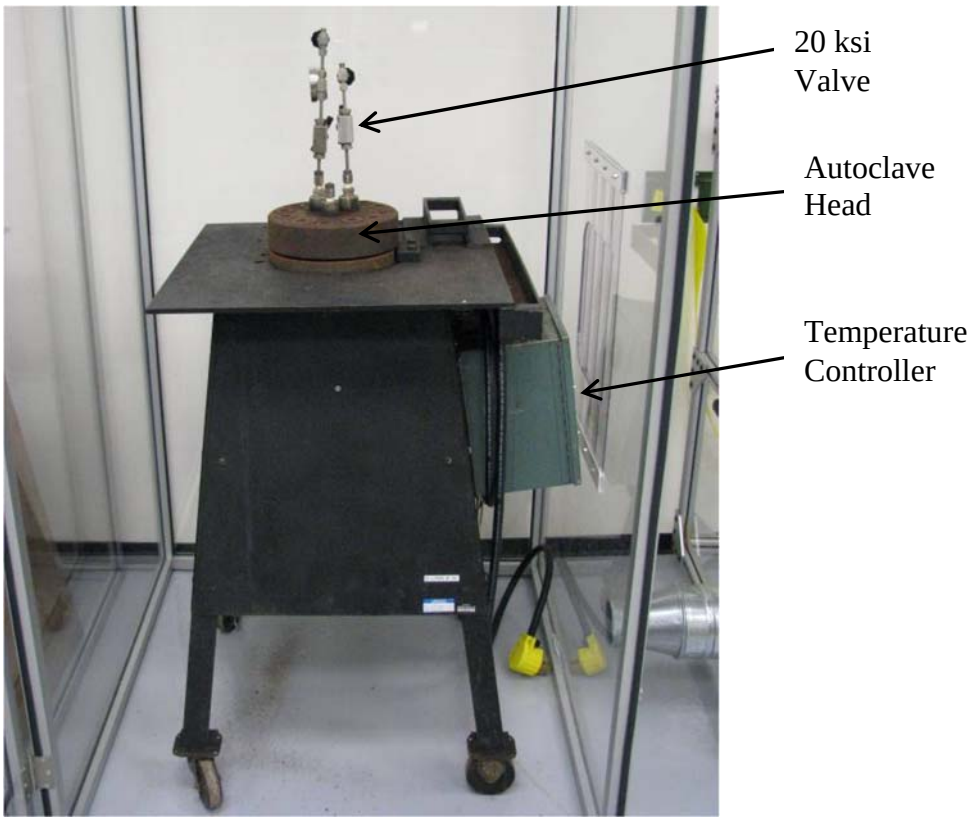

Figure 1. Autoclave Apparatus (5-Liter, 5000 psig)

3.2 Corrosion Specimens

Figure 2 shows the corrosion specimen test rack that was positioned in the headspace of the autoclave. This rack shows two kinds of specimens, U-bends and corrosion coupons. U-bends are 1-inch x 5-inch x 1/8 inch strips bent around a 1-inch diameter mandrel into a U-shape. U-bends represent the worst-case stress corrosion cracking (SCC) specimen due to the high plastic stresses in the bent region. The corrosion coupons were 1-inch x 1-inch x 1/8-inch with a centered 0.280 mounting hole with a 120-grit surface finish in compliance with ASTM G1.

The specimens were mounted on the test racks using TFE shoulder washers to electrically isolate the specimens from the rack and each other. Electrical isolation was verified by Fluke meter. Each rack was equipped with the following:

- Three U-bends each of X65 carbon steel, Type 316L stainless steel, and Type 410 (13Cr) stainless steel;
- One U-bend of 4130 steel (known to be susceptible to sulfide stress cracking (SSC); and
- Three flat corrosion coupons each of X65 carbon steel, Type 316L stainless steel, and Type 410 stainless steel.

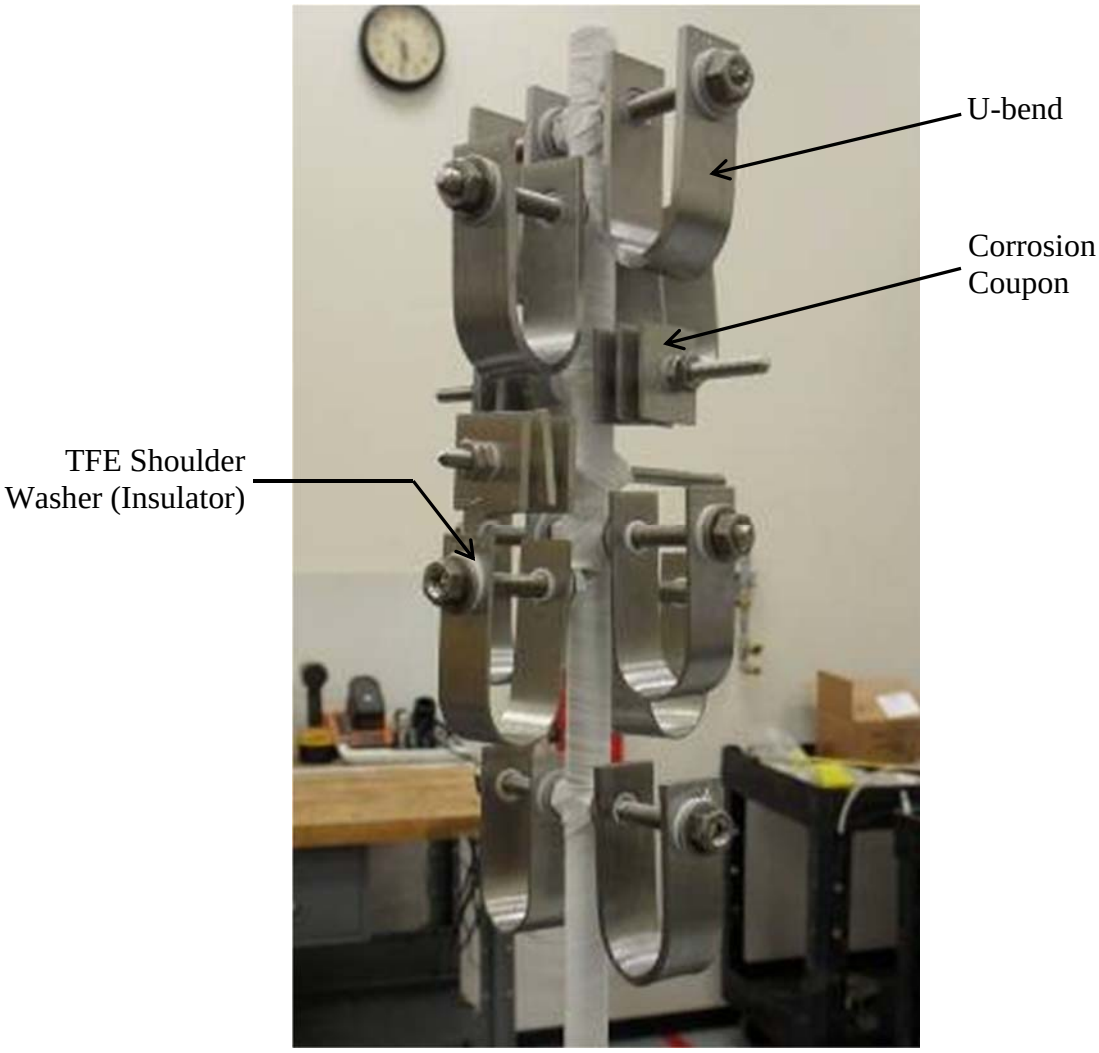

Figure 2. Test Rack

3.3 Autoclave Configurations

Figure 3 shows the two autoclave configurations that were used during the test program. As shown in the figure, the specimen section of the test rack was positioned in the headspace of the autoclave with a small reservoir of humidifying solution in the bottom of the autoclave. In Configuration A, surges of CO_2 from the booster pump required to pressurize the autoclave to 1275 psig splashed the humidifying solution throughout the headspace. This configuration was used for the first six tests before this effect was recognized when deposits of sodium chloride salts were found on the specimens in Tests 5 and 6. Configuration B resolved this problem and was used for Tests 7-13. Configuration A was used intentionally for the four methanol/water tests where it was desired that the specimens be splashed with the humidifying solution.

A rain hat and splatter guard was added to the test rack for Tests 5-13. The purpose of the rain hat was to prevent water droplets that may have condensed on the lid of the autoclave from dropping down onto the specimen rack. The rain hat and splatter guard were not used for the methanol-water tests that required liquid wetting of the specimens.

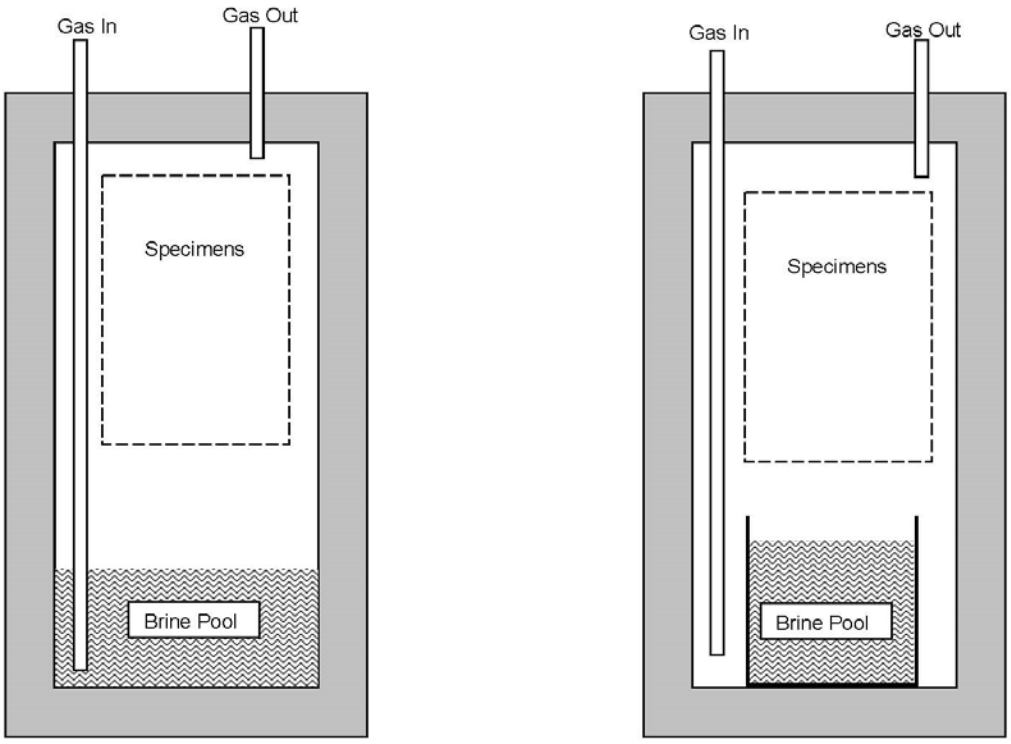

Configuration A **Configuration B**

Figure 3. Autoclave Configurations Used During the Test Program

3.4 Procedures for Loading the Autoclaves and Evaluation of Test Specimens

The procedures for loading the autoclaves are described in detail in the published research report[1] for this work. It should be noted, however, that two methods were used to charge the H_2S into the autoclaves for the first six tests: a liquid loading method in which a known weight of liquid H_2S was injected into the autoclave, and a gas-pressurized loading method in which the autoclave was pressurized to a pre-calculated level. During Test 5, it was determined that the gas-pressurized loading method did not result in the desired H_2S concentration in the vapor phase while the liquid loading method in Test 6 did. The autoclave for Test 5 was purged and recharged using the liquid loading method. The H_2S concentrations were also conservatively recalculated for Tests 2 and 4 (initially done with the gas-pressurized loading method) and the liquid loading method was used for all subsequent H_2S tests.

The coupons for each test were cleaned and measured using standard methods described in the research report[1]. The corrosion rate was then calculated by the following equation:

$$\text{Corrosion rate (mpy)} = 534(m)/(DAT)$$

Where: m is the mass loss, milligrams
D is the density, g/cm^3
A is the area, inches^2
T is the exposure time, hours

After cleaning, the coupons were inspected by stereomicroscope for pitting and crevice corrosion. Pit and crevice depth were measured optically on the metallograph using the focal plane method. The U-bends were also examined by stereomicroscope for indications of cracking.

4.0 DISCUSSION OF RESULTS

The experimentally measured, average corrosion rates for all 17 autoclave tests are presented in the figures and text below. More detailed results and discussion, including the corrosion rates for individual specimens and other experimental observations are provided in the appendices of the research report[1] for this work. The experimental accuracy and precision of measurements are also discussed in the research report[1].

The tests are numbered in the order they were performed. The first series of four tests were conducted at 100% RS to determine if significant corrosion would be observed at this condition. If so, then subsequent tests were conducted to establish a practical maximum RS level at which corrosion would not be significant. The results are shown in "mils per year" (mpy), which is equivalent to 0.001 inch/yr or 0.0254 mm/yr.

4.1 Effect of H_2S and Temperature on Corrosion at 100% Relative Saturation

Figure 4 shows the corrosion rate results for Tests 1-4 and Test 8 at 100% relative saturation with distilled water. Tests 1 and 3 without H_2S at 125°F and 75°F had carbon steel corrosion rates of 0.87 and 0.39 mpy, respectively. When H_2S was present, the carbon steel corrosion rates were up to one order of magnitude greater in dense-phase CO_2 at 75°F for Test 4 (12.4 mpy) than under supercritical conditions at 125°F for Test 2 (1.34 mpy). This trend was not observed in the absence of H_2S. Pitting was detected in Tests 1, 3, and 4. Crevice corrosion did not occur for Tests 1-4.

The 410 and 316L stainless steel corrosion rates were generally less than 0.6 mpy for Tests 1-4, and the corrosions rates did not vary as significantly with changes in H_2S content and temperature. Some cracking was observed with the 316L U-bends observed in Test 2, and pitting in Tests 1 and 2. Stainless steel 410 only experienced pitting in Test 2. Crevice corrosion was not observed for any of the stainless steel samples.

Test 8 was conducted as a repeat of Test 2, but without allowing the distilled water to splatter on the specimens. The purpose of Test 8 was to see if the cracking of Type 316L observed in Test 2 could be reproduced. Both U-bend specimens and C-ring specimens stressed at 100% of their specified minimum yield stresses were included in this test. The result of Test 8 was that average corrosion rates of 1 mpy or lower were observed for all specimens and no pitting or crevices were observed. None of the Type 316L U-bends or Type 316L C-Rings exhibited cracking. It is suspected that the U-bends in Test 2 could have been cracked during stressing prior to exposure.

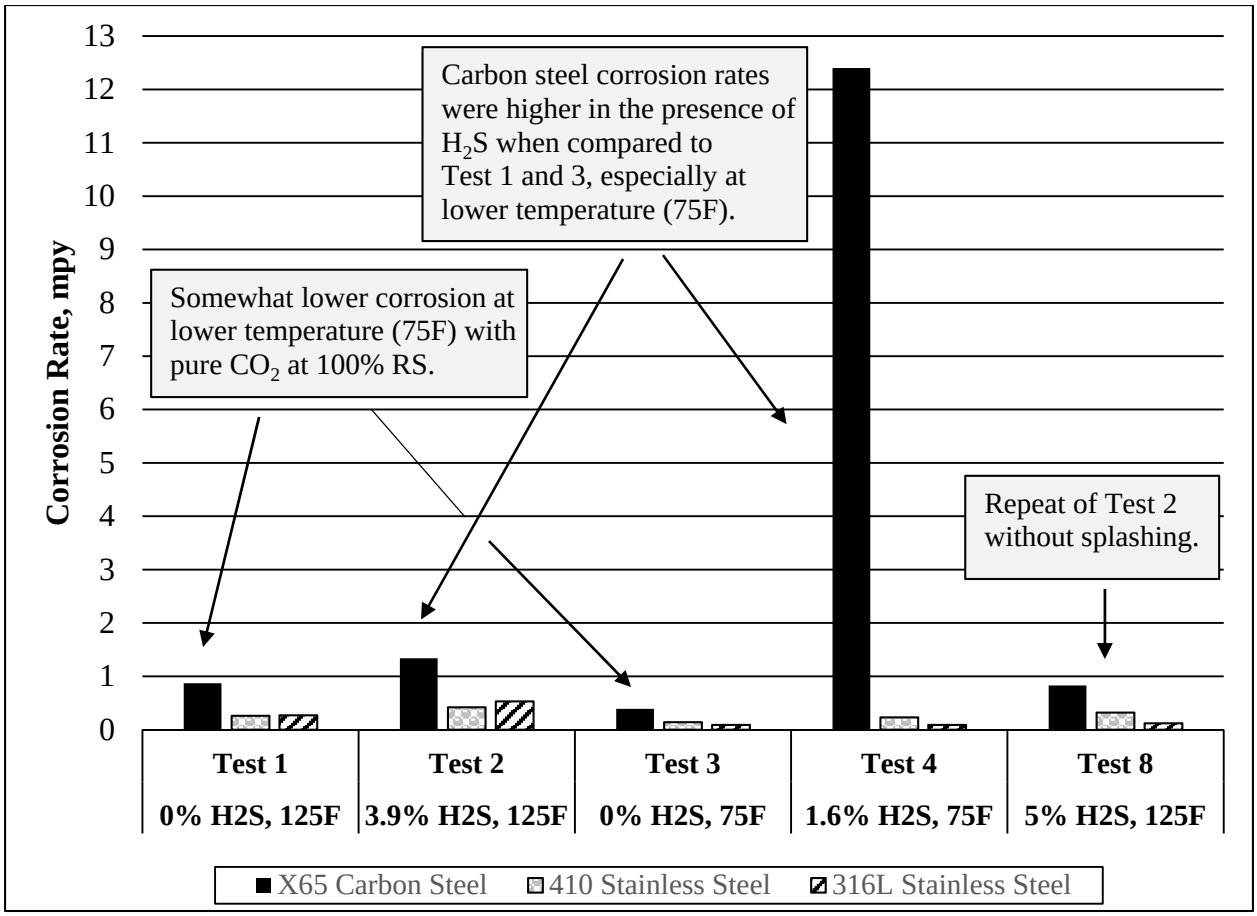

Figure 4. Effect of H_2S and Temperature on Corrosion Rates at 100% RS

4.2 Effect of H_2S and Temperature on Corrosion at 75% Relative Saturation

Figure 5 shows the corrosion rate results for Tests 5-7 and 9. Based on the observation that the most severe corrosion in Tests 1-4 occurred in the presence of H_2S, Tests 5 and 6 were conducted with the 5% H_2S test condition and at the 75% RS level to determine if the lower moisture levels would eliminate the pitting corrosion observed in the previous tests. However, it was during these tests that it was determined that autoclave Configuration A (see Figure 3) was inadvertently splashing the specimen samples with the humidifying salt solution. These specimens were contaminated with deposits of NaCl salts. Given that NaCl films are hygroscopic, it is possible that more corrosion occurred in Tests 5 and 6 than would have occurred in the absence of NaCl.

Therefore, Test 7 was a repeat of Test 5, but with dry corrosion specimens. Test 7 indicated a carbon steel corrosion rate of 0.16 mpy, which is lower than the corrosion observed with Test 5 (0.35 mpy). The carbon steel corrosion rate in Test 7 was also lower by a factor of 8 compared to Test 2 at 1.34 mpy. None of the U-bends showed cracking during Test 7. No pitting or crevice corrosion was observed either.

Despite the fact that the specimens from Test 6 (0.72 mpy) were contaminated with salt, reducing the relative humidity to 75% reduced the carbon steel corrosion rate by more than one order of magnitude compared to Test 4 (12.4 mpy) at 75°F and 100% RS.

Test 9 was conducted at 125°F and 75% RS without any H_2S. This is essentially the same test condition as Test 7 but without the H_2S. No statistically significant corrosion was observed and no crevice corrosion, cracking, or pitting was observed for any of the samples.

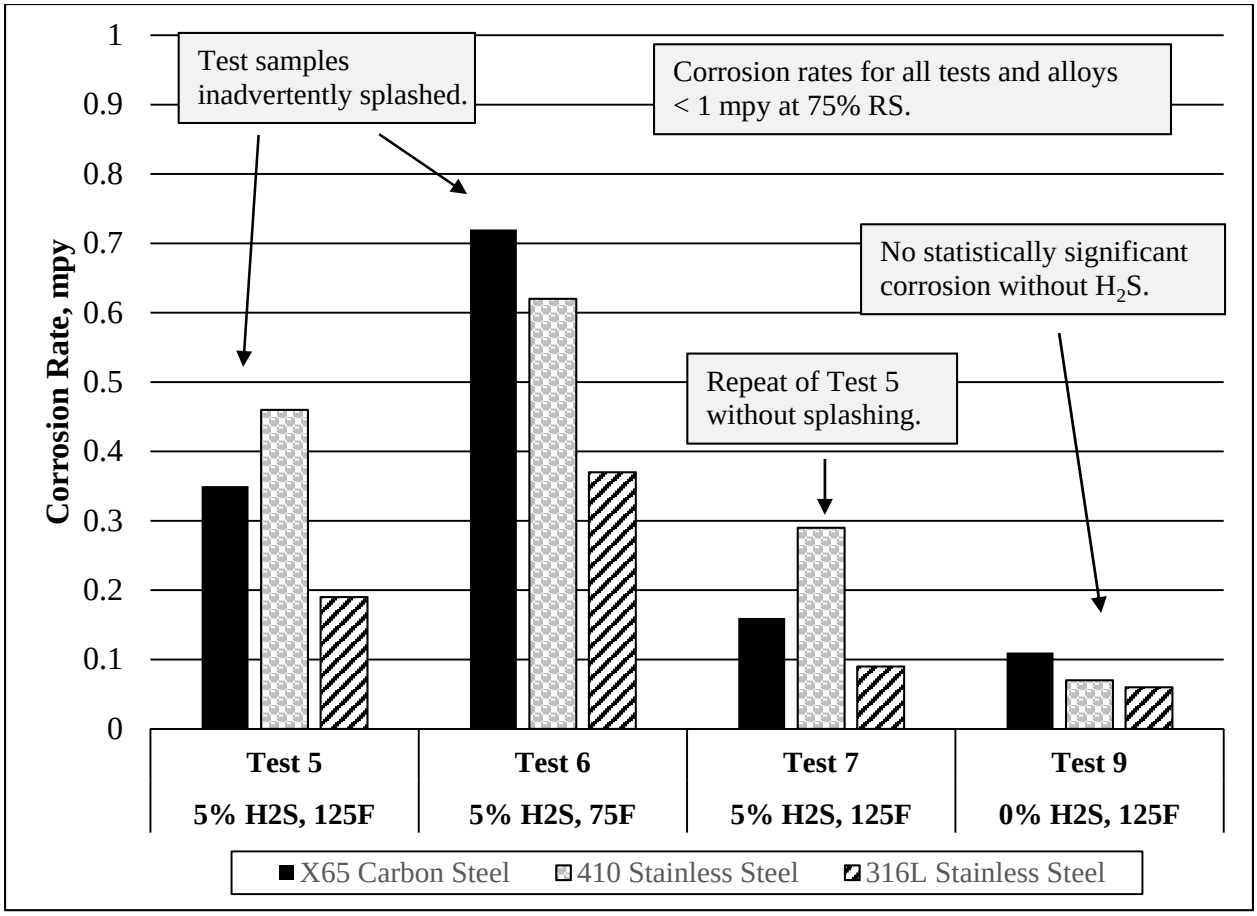

Figure 5. Effect of H_2S and Temperature on Corrosion Rates at 75% RS

4.3 Effect of O_2 and Temperature on Corrosion at 75% Relative Saturation

Figure 6 shows the corrosion rate results for Tests 10-13. Test 9 was discussed in the previous subsection and is also shown here for comparison to Tests 10-13. Test 10 was designed to determine whether carbon steel corrosion rates were higher at 75°F than at 125°F at the 75 % RS condition with pure CO_2. This was done because Test 2 and Test 4, both with H_2S at 100% RS, showed a lower corrosion rate at 125°F than at 75 °F, which was an unexpected result. With pure CO_2 at 75% RS, the carbon steel corrosion rate was 0.42 mpy at 75°F (Test 10) and 0.11 mpy at 125°F (Test 9).

Test 11 was designed to examine the effect of having 1 mol% oxygen in the gas at the 75% RS level. Comparison of the results of Test 11 with those of Test 9 show that while there was a statistically significant increase in corrosion rates, the corrosion rates for all materials in both Test 9 and Test 11 were less than 0.5 mpy. No pitting or crevice corrosion was observed, and none of the U-bends exhibited cracking.

Both Test 10 and 11 were repeated as Tests 12 and 13 due to concerns over the lack of any significant differences in corrosion observed in Tests 10 and 11 and the lack of any difference between carbon steel or stainless steel, and the lack of any effect of oxygen. Tests 12 and 13 did show a statistically significant increase in corrosion resulting from the addition of oxygen in Test 13, but the corrosion rates of all three alloys tested at 75% RS in Test 13 were less than 0.5 mpy. Test 12 essentially reproduced the results of Test 10.

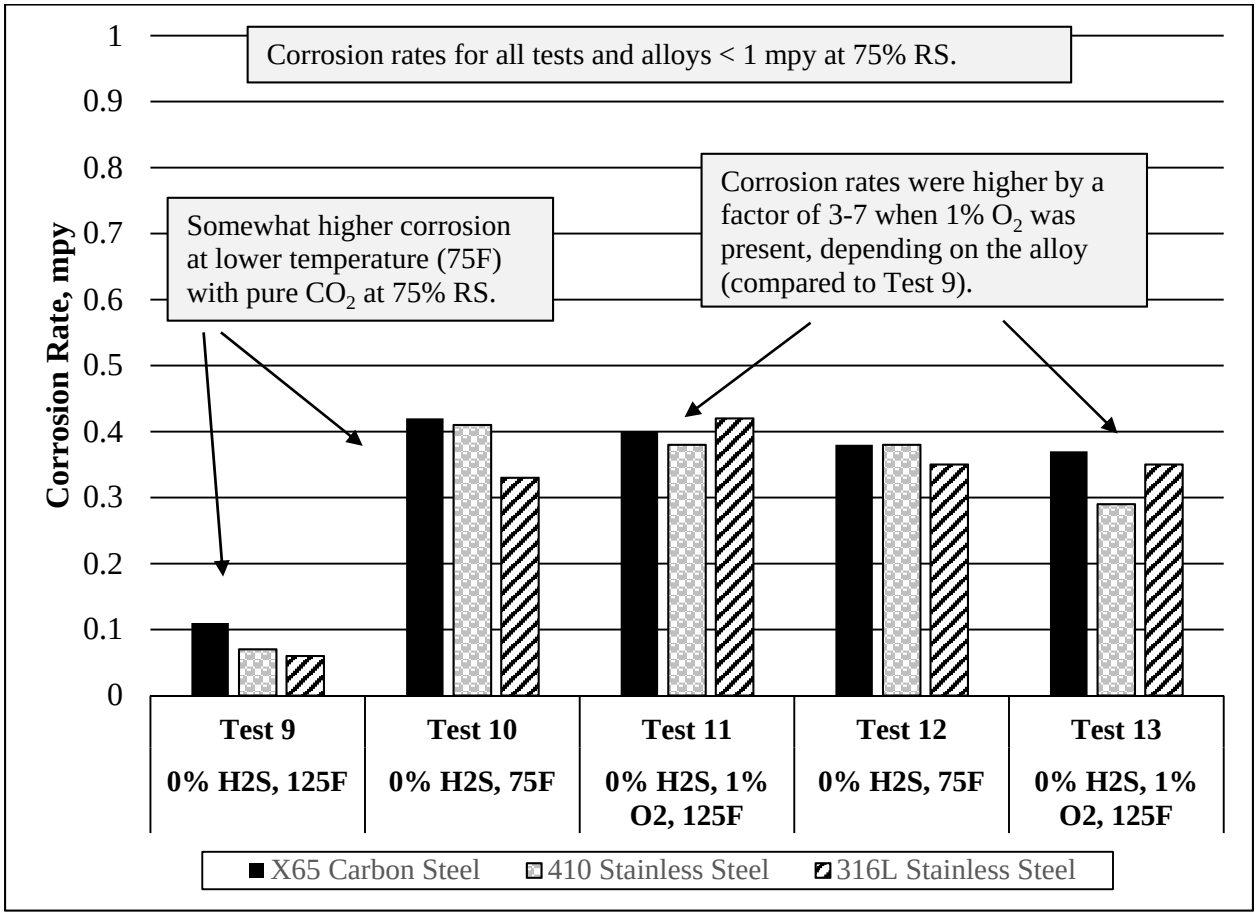

Figure 6. Effect of O_2 and Temperature on Corrosion Rates at 75% RS

4.4 Effect of Methanol-Water Film, H_2S, and O_2 on Corrosion at 100% Relative Saturation

Figure 7 shows the corrosion rates for Tests 14-17. These tests examined the effect of 20 wt% methanol-water solutions, with and without the presence of H_2S and/or oxygen. Twenty percent methanol was selected as representing a probable worst case from the standpoint of corrosion. These last four tests were all conducted at 75ºF because it was deemed less likely that methanol would be present at the higher temperatures since it is typically used to inhibit hydrate formation. The tests were also performed using Configuration A shown in Figure 3 to splatter the specimens with the methanol-water solution; it was desired to test the worst case corrosion, and it was thought that the worst corrosion in a pipe with methanol injected for hydrate inhibition would likely occur at the bottom of the pipe, where a liquid methanol-water phase might form.

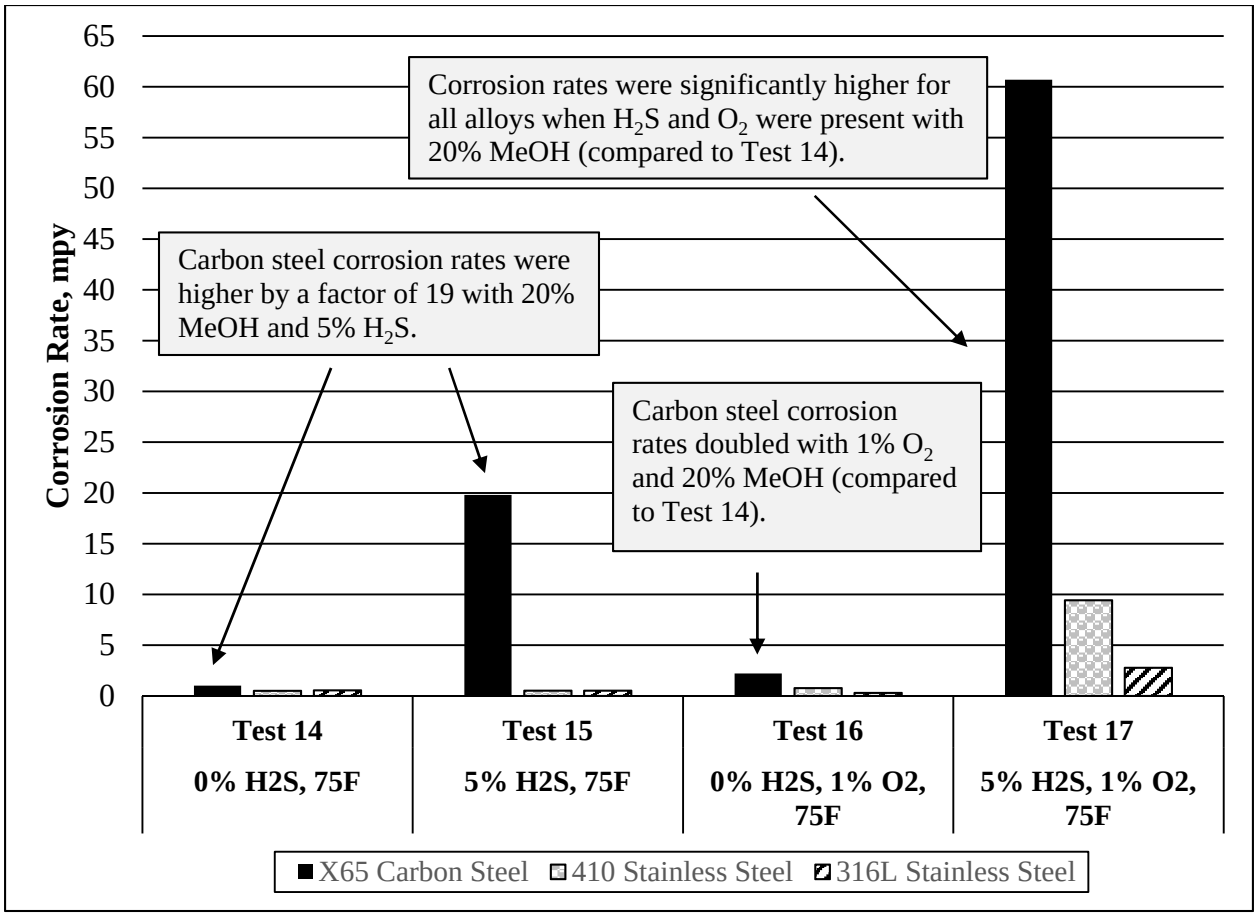

Figure 7. Effect of Methanol-Water Film, H_2S and O_2 on Corrosion Rates at 100% RS

Test 14 showed essentially a doubling of the corrosion rate for carbon steel when methanol solution was present (1.02 mpy), compared to Test 3 (0.39 mpy) at the same conditions but without methanol. Test 15 showed an approximate 50-fold increase in carbon steel corrosion rate (19.8 mpy) when compared to Test 3. Test 16, which included oxygen but no H_2S, resulted in a 6-fold increase in the carbon steel corrosion rate (2.21 mpy). Test 17, with both oxygen and H_2S, exhibited severe corrosion at 60.7 mpy, a 155-fold increase compared to Test 3. The surface was severely corroded with distinct pits for Tests 15 and 17; Test 16 demonstrated pitting to a lesser extent.

The 410 and 316L stainless steel tests did not experience significant corrosion until both H_2S and O_2 were evaluated with the methanol solution. Then, the 410 stainless steel corrosion rate was 9.43 mpy and the 316L stainless steel corrosion rate was 2.77 mpy. For all of the other tests, corrosion of the stainless steel alloys was less than 1 mpy. Pitting occurred for Tests 15-17 with 410 stainless steel and during Test 17 for 316L stainless steel.

5.0 CONCLUSIONS

The main conclusion for the test program is that for all tests conducted with mixtures of CO_2, with up to 5% H_2S and/or 1% oxygen at 1275 psig, the corrosion rate measured for all of the X65 carbon steel alloys tested was less than 1 mpy when the relative water saturation was held at 75%. For tests conducted at 100% relative saturation of water, or in the presence of a mixture of 20 wt% methanol in water, the corrosion rates were significantly higher. Other more specific conclusions are discussed below:

- At 100% relative saturation, the presence of H_2S at the concentrations used significantly increased the corrosion rate of carbon steel. Carbon steel corrosion rates were up to one order of magnitude greater in dense-phase CO_2 than under supercritical conditions at 125°F when H_2S was present. This trend was not observed in the absence of H_2S.

- At 75% relative saturation, the corrosion rate was less than 1 mpy without pitting for any of the alloys even when oxygen or H_2S was present.

- The effect of the methanol-water liquid film at 75°F was that the corrosion rate doubled for carbon steel in dense-phase CO_2. The addition of 5 mol% H_2S without O_2 resulted in a 50-fold increase in carbon steel corrosion rates. The addition of 1 mol% O_2 without H_2S resulted in a 6-fold increase in carbon steel corrosion rates. Lastly, the addition of both H_2S and O_2 resulted in a 155-fold increase in carbon steel corrosion rates.

In general, the test program provided many useful insights into the types and levels of corrosion that may occur for different alloys at the high pressure, high H_2S operating conditions typical of AGI and CCS units. Additional tests may need to be performed to expand on some of the trends observed in this study, and the evaluation of the effects of other parameters may be warranted. If additional research is conducted, it may be possible to develop an empirical model or correlation that could be used to predict corrosion rates as a function of process conditions. This would help industry leaders identify safe operating conditions and better design systems for handling high pressure CO_2 streams at minimal cost with appropriate materials.

6.0 ACKNOWLEDGEMENTS

The authors would like to acknowledge the Gas Processors Association for their expertise, management, and support for this project. The project coordinator, Scott Northrop, also provided important oversight and management for the project. The laboratory equipment provided by Honeywell Corrosion Solutions was also an invaluable resource for conducting the research required for this study.

7.0 REFERENCES

1. McIntush, K.; K. Fisher; and P. Ellis. "Corrosion in Acid Gas Injection Systems", GPA Research Report, RR-222, GPA Project 101, June 2014.